Heteropolyacid supported on Zr-Beta zeolite as an active catalyst for one-pot transformation of furfural to γ-valerolactone

Haryo Pandu Winoto[a], Zuhroni Ali Fikri[a,b], Jeong-Myeong Ha[a,b], Young-Kwon Park[c], Hyunjoo Lee[a,b], Dong Jin Suh[a], Jungho Jae[a,d,*]

[a] Clean Energy Research Center, Korea Institute of Science and Technology, Seoul 02792, Republic of Korea
[b] Division of Energy and Environment Technology, KIST School, Korea University of Science and Technology, Seoul 02792, Republic of Korea
[c] School of Environmental Engineering, University of Seoul, Seoul 02504, Republic of Korea
[d] School of Chemical and Biomolecular Engineering, Pusan National University, Busan 46241, Republic of Korea

ARTICLE INFO

ABSTRACT

A novel bifunctional catalyst that enables an efficient one-pot conversion of furfural into γ-valerolactone (GVL) has been developed by anchoring heteropolyacid (HPA) on Zr-Beta zeolite. The catalysts were prepared by a post-synthesis procedure, which consists of the dealumination of Al-Beta, incorporation of Zr into the beta framework through solid-state ion-exchange and impregnation of the HPA. Zr-Beta is used as a Lewis acid catalyst to catalyze the transfer hydrogenation of furfural and levulinic acid/ester using 2-propanol as a hydrogen donor. To deal with the inability of Zr-Beta to catalyze the hydrolytic ring-opening of furans toward GVL, phosphotungstic acid (HPW) and silicotungstic acid (HSiW) were introduced to the Zr-Beta as BrØnsted acid sites. The characterization of the catalysts using XRD, UV–vis and XPS as well as TPD of ammonia and FT-IR spectroscopy of the adsorbed pyridine revealed that the HPA/Zr-Beta possesses both isolated Lewis and BrØnsted acid sites. When they were applied to the one-pot cascade conversion of furfural, the initial activity of the HPA/Zr-Beta toward GVL production were 2–3 times greater than that for Zr-Beta due to the enhanced hydrolytic ring-opening of the furans promoted by the added BrØnsted acidity. Especially, HPW loaded Zr-Beta demonstrated a remarkable GVL yield of ~70% at 433 K after 24 h due to its high thermal stability and stronger BrØnsted acidity, and its activity far surpasses that of the conventional Sn-Al-Beta zeolite (~40%). Overall, this study demonstrates that an incorporation of HPA into Lewis acid Sn- or Zr-Beta zeolites is an effective strategy to create isolated Lewis and BrØnsted acid sites within a single catalyst, thereby allowing the selective cascade catalysis for the cost-effective production of high-value chemicals.

1. Introduction

The depletion of fossil fuels and global climate change have motivated our society to develop renewable energy technologies that can reduce our dependence on fossil fuels. Among the various renewable energy resources, lignocellulosic biomass is regarded as a viable alternative to petroleum-derived liquid fuels and chemicals due to its abundance and carbon neutrality [1,2]. Lignocellulosic biomass typically contains 30–50 wt % of cellulose and 20–30 wt % of hemicellulose depending on its source [1]. These cellulosic portions of the biomass can be easily depolymerized into furanic compounds such as furfural and 5-hydroxymethylfurfural (HMF) under aqueous acidic conditions [3–6]. Therefore, furfural has been extensively studied as a platform chemical for the production of a range of liquid fuels such as diesel and

jet fuel range alkanes [7], and chemicals such as γ-valerolactone (GVL) [8,9] and BTX-aromatics [10,11]. Especially, GVL, as one of the furfural-derived chemicals, has emerged as a versatile molecule which has various applications ranging from a polymer precursor to a green solvent [8,12].

The production of GVL from biomass-derived carbohydrates involves multiple reaction steps which consist of the acid-catalyzed dehydration of sugar, the hydrogenation of furfural, the acid-catalyzed ring-opening of furfuryl alcohol (FA), and finally the hydrogenation of levulinic acid (LA) or its esters to GVL [8,13,14]. Although each single step has been optimized by various heterogeneous catalysts and process conditions, the direct production of GVL from biomass in a one-pot fashion is highly desirable to reduce the number of unit operations and thereby the process cost. Especially, the application of the Meerwein-

Ponndorf-Verley (MPV) reduction pathway to GVL production paves the way for the development of a one-pot process [15]. Instead of using noble metal catalysts (e.g., Pd) and high-pressure H_2, the transfer hydrogenation pathway, such as MPV reduction, enables the selective hydrogenation of LA or furfural to the corresponding products over cheap metal oxides with Lewis acid-base properties using secondary alcohols (e.g., 2-butanol) as a hydrogen donor [16–19]. Among a variety of metal oxide catalysts, Lewis acid Sn- or Zr-Beta zeolites have been shown to be remarkably active and selective for the MPV reactions of furfural and LA derivatives [19–21]. Therefore, acid chemistry such as a ring-opening reaction of FA can be easily combined with reduction chemistry using heterogeneous catalysts loaded with well-balanced Brønsted and Lewis acid sites.

Bui et al. first demonstrated the one-step conversion of furfural to GVL using a physical mixture of Zr-Beta and mesoporous Al-MFI zeolites as Lewis and Brønsted acid catalysts, respectively [13]. The mixture catalyst system achieved a decent GVL yield of ∼68% at 393 K after a 24 h reaction time. Following their work, in an attempt to improve the catalyst selectivity and reusability, several researchers studied single zeolite catalysts with both Lewis and Brønsted acid functionalities for the one-pot conversion of furfural [22–26]. Antunes et al. first reported on the application of a bifunctional Sn-Al-Beta zeolite with both Lewis acid Sn and Brønsted acid Al in the framework to the furfural conversion [22]. The catalyst was synthesized via a post-synthesis route which started from dealumination of the commercial H-Beta followed by incorporation of both Sn and Al active sites into vacant T sites by solid-state ion-exchange (SSIE). Although the synthesized Sn-Al-Beta exhibited high activity for furfural conversion, the catalyst was only selective toward furfuryl alkyl ether (FE), which is an intermediate compound of LA, and no GVL was produced at 393 K. Later, our research group optimized the acid properties of Sn-Al-Beta zeolite by adjusting the Sn/Al ratio and the tin incorporation method (e.g., the use of an organometallic tin precursor). We demonstrated that an improved GVL yield of 60% could be achieved using the Sn-Al-Beta zeolite with a Sn/Al ratio of 6.5 at 453 K after 24 h, highlighting the importance of a well-balanced Lewis/Brønsted acidity for efficiently promoting both the MPV and hydrolysis reactions [23]. More recently, Melero et al. reported on the direct production of GVL from C5 sugars such as xylose using a bifunctional Zr-Al-Beta zeolite [24]. The optimized catalyst with an Al/Zr ratio of 0.20 successfully produced GVL with a yield of 34% at 463 K after a 10 h reaction. Later, Song et al. reported that an introduction of mesoporosity to the Zr-Al-Beta could allow to achieve the high-yield conversion of furfural to GVL over 90% at 393 K and 24 h reaction time [9].

Overall, bifunctional Sn(Zr)-Al-Beta zeolites have shown promise for the integrated conversion of furfural to GVL, but the overall activity and GVL selectivity are somewhat lower than that over the mixture catalyst of Zr-Beta and Al-MFI zeolites. In addition, the need for a high catalyst loading (e.g., a typical catalyst to reactant ratio of 1–4) to complete the reaction is a significant barrier for their application to industrial-scale production. In the post-synthesis bifunctional zeolite system, it is difficult to incorporate large amounts of Al and Sn (or Zr) into the zeolite framework simultaneously due to the limited availability of silanol nests (i.e., T sites). Indeed, our previous investigation revealed that the selective incorporation of Sn atoms into the beta framework with high Al content via the SSIE technique is highly challenging, creating Sn species mostly located at extra-framework positions [23]. Therefore, instead of using the internal Al atoms as the source of Brønsted acidity, we conceived of the concept of introducing a new external Brønsted acid source, which does not depend on the silanol nest, to Lewis acid Sn or Zr-Beta catalysts to improve their bifunctional sites.

Keggin-type heteropolyacids (HPAs), such as phosphotungstic acid (HPW) and silicotungstic acid (HSiW), are known as highly active catalysts for a range of acid-catalyzed reactions such as dehydration and etherification due to their strong Brønsted acidity [27–30]. Keggin

HPAs possess the general formula $H_n[XM_{12}O_{40}]^{n-}$, wherein X is the central atom within the cage (X = P^{5+}, Si^{4+}, Al^{3+}, etc.) and M is the addenda atom (M = W or Mo), and their acid strength varies depending on which metal is used [29]. Among the various Keggin HPAs, HPW and HSiW were reported to possess stronger Brønsted acidity than do zeolites and other acidic oxides [28]. HPAs are typically supported on various metal oxides (e.g., SiO_2, ZrO_2, TiO_2) to improve their low surface area[31]. Silica is especially known as a suitable support to keep the strong Brønsted acid character of HPAs due to the weak metal-support interaction [11]. Therefore, HPAs supported on zeolite beta matrix can serve as strong acid sites which are comparable to the framework Al sites.

In this work, we report the synthesis and characterization of a novel bifunctional catalyst of heteropolyacid (HPA) anchored on Zr-Beta zeolite and its application to the integrated conversion of furfural to GVL. By utilizing Keggin HPAs (i.e., HPW, HSiW) as a source of Brønsted acidity, the silanol nests of the dealuminated beta can be fully occupied by Zr, thereby allowing for the optimal loading of both Brønsted and Lewis acid sites within a single catalyst. Beneficial effects of HPA addition are thoroughly probed via acid titration techniques and short-time reaction assessment from selected intermediates. Of the prepared catalysts, HPA loaded catalysts are capable of suppressing the formation of furfuryl ether as a recalcitrant intermediate. Furthermore, HPA and Zr-active sites are capable of working synergistically, increasing the GVL production rate from LA significantly. Eventually, we demonstrate a remarkable GVL yield of ∼70% under mild conditions (433 K, 24 h and a catalyst to furfural ratio of 0.8) using a single HPA/Zr-Beta catalyst.

2. Experimental

2.1. Materials

The following chemicals were used as received from the suppliers: furfural (98%, Sigma), 2-propanol (99%, Sigma), furfuryl alcohol (99%, Sigma), levulinic acid (99%, Alfa), 5-methyl furanone (98%, Alfa), γ-valerolactone (98%, Alfa), ethyl levulinate (99%, Sigma), nitric acid (64–66 %, Sigma), zirconocene dichloride (99%, Alfa), phosphotungstic acid (99.9%, Sigma), silicotungstic acid (99.9%, Sigma).

H-Al-Beta (Zeolyst CP814E, Si/Al = 12.5) was calcined at 773 K for 4 h in the box furnace prior to its use. The calcination procedure was intended to change the cation form from NH_4^+ to H^+.

2.2. Catalyst preparation

Dealumination of H-Al-Beta was conducted in a highly-concentrated HNO_3 solution (65 wt %) at 353 K for 24 h to fully remove Al in the zeolite [23,32]. The mixing ratio of H-Al-Beta to HNO_3 solution was fixed to 1 g: 20 ml solution. After dealumination process, suspended solid was recovered, washed with deionized water copiously, and dried at 373 K overnight. The dried sample was then calcined at 773 K in a box furnace for 4 h to completely remove NO_3^- species. Subsequently, the calcined sample was denoted as Si-Beta.

Zr-Beta zeolite was prepared by the SSIE method described elsewhere [33]. Briefly, Si-Beta zeolite was homogenized with Zr-precursor (zirconocene dichloride) in a dry environment with a typical loading amount of 5 wt% Zr. This mixture powder was then calcined under flowing air in a tubular furnace at 823 K for 6 h and denoted as Zr-Beta. Keggin structure heteropolytungstates of phosphotungstic acid ($H_3[P(W_3O_{10})_4]$) and silicotungstic acid ($H_4[Si(W_3O_{10})_4]$) was loaded on Zr-Beta or Si-Beta through incipient wetness impregnation following the procedure similar to our previous work [11]. After impregnation, HPA loaded samples were denoted as HPW (or HSiW)/Si-Beta and HPW (or HSiW)/Zr-Beta for HPA loaded dealuminated zeolite beta and Zr-Beta, respectively.

2.3. Catalyst characterization

Powder X-Ray Diffraction (XRD) patterns were obtained using a LabX XRD 6000 with a Cu source. Bulk compositions of the catalysts were measured by using an inductively coupled plasma atomic emission spectroscopy (ICP-AES, Polyscan-61E). Porosity characterization of the catalysts were conducted with a BELSORP-mini II gas adsorption analyzer using N_2 gas. Samples were pretreated at 523 K under vacuum before N_2 adsorption. The obtained adsorption-desorption data were analyzed using the Brunauer-Emmett-Teller (BET) and t-plot method to calculate specific surface area and microporous volume, respectively. The surface composition and electronic state of Zr and W in the prepared catalysts were measured by X-ray photoelectron spectroscopy technique using a Shimadzu ESCALAB 250 instrument equipped with a monochromatic X-ray source of Al Kα. Diffuse reflectance UV–vis spectra of the catalyst samples were recorded in the region of 200–500 nm using a Cary 5000 spectrophotometer. The obtained UV–vis spectra were transformed into Kubelka-Munk unit to characterize both intraframework Zr species and Keggin structure [34]. Energy dispersive X-ray spectroscopy (EDX) mapping images were obtained using a Hitachi FE-SEM S-4100 equipped with cold field emission gun.

Total acidity of the catalysts was analyzed by temperature-programmed desorption (TPD) of NH_3 in a BELCAT-B catalyst analyzer connected with TCD and BELMass-MS detector. Prior to NH_3 adsorption, the catalysts were pretreated in flowing He at 523 K for 2.5 h. After the samples being stabilized at 393 K, NH_3/He mixture gas was exposed to the samples in a flow rate of $8.0\ cm^3$/min for 0.5 h. The amounts of desorbed ammonia in the temperature region of 393 K–823 K were then used to assess the total acidity of the samples. The nature of surface acidity in the catalysts was analyzed by pyridine-adsorbed Fourier transform infrared spectroscopy (FTIR) in a JASCO FT-IR/4100 equipped with Harrick high temperature cell and CaF_2 window. Before analysis, each sample was pretreated under vacuum in 523 K for 2.5 h. Subsequently, pyridine was adsorbed onto the sample at 323 K for 15 min. The sample was degassed at 423 K for 0.5 h to remove any physically adsorbed pyridine molecules, and the peak areas at $1450\ cm^{-1}$ and $1548\ cm^{-1}$ were used to quantify the ratio of Lewis to BrØnsted acid sites.

2.4. Catalytic reaction test

Catalytic performance tests of the prepared catalysts were conducted in two ways. As the first approach, the assessment of catalytic activity was conducted using several intermediates as a reactant in a short reaction time to observe the intrinsic activity of individual active sites without any diffusion limitations. Next, the one-pot transformation of furfural into GVL was conducted over extended reaction time to evaluate the beneficial aspect of HPA addition onto Zr-beta zeolite toward a GVL production.

2.4.1. Short-time reaction experiments

A typical reaction was conducted in a 90 ml stainless steel reactor loaded with 0.11 M of selected intermediates (i.e. furfuryl alcohol or levulinic acid) in 20 ml of 2-propanol (i.e., isopropanol, IPA) with a catalyst amount of $4\ g_{cat}\ L^{-1}$ loading. Prior to the catalytic reaction test, the reactor was purged with N_2 gas to remove air and pressurized to 10 bar. The reactor was then heated to the desired temperature (393 K) and kept isothermally for 1.5 h under vigorous mixing by a magnetic stirrer. Product distribution of every catalytic reaction was analyzed by using gas chromatography-flame ionization detector (GC-FID, Agilent GC 7890B) with HP-5 column, while chemical structure of each product was determined by using GC–MS (Agilent GC 5890) with the same column. Quantification of products was carried out by measuring the FID signal response factors of pure commercial chemicals. The performance of each catalyst is expressed as the productivity rate

and calculated with the following equation:

$$Productivity\ rate\ (mmol \cdot h^{-1}) = \frac{Amount\ of\ formed\ product\ (mmol)}{Reaction\ time\ (h)}$$

2.4.2. Full catalytic reaction assessment

Similar to the previous procedure, a reactor was charged with 0.11 M of furfural in 20 ml of 2-propanol and with varying amounts of catalysts ($8–10\ g_{cat}\ L^{-1}$). The reaction was conducted at the temperature of 413–433 K and with varying reaction times of 2–24 h under vigorous mixing by a magnetic stirrer. Product quantification was done in the same way with the short-time reaction analysis. The catalytic performance of each catalyst is expressed as the yield of both GVL and intermediate products with the following equation:

$$Yield\ (\%) = \frac{Amount\ of\ product\ formed\ after\ reaction\ (mol)}{Amount\ of\ furfural\ fed\ in\ the\ reactor\ (mol)} \times 100\ \%$$

3. Results and discussion

3.1. Catalyst characterization

To completely remove the Al atoms from H-Al-Beta and generate free silanol nests to anchor the Zr atoms, a strong acid solution (14 M HNO_3) was employed for the dealumination step [32]. The effect of various catalyst preparation processes (i.e., dealumination, Zr incorporation and HPA impregnation) on the zeolite beta crystal structure was initially investigated using XRD analysis, as shown in Fig. 1. The acid treated zeolite beta (i.e., Si-Beta) still possessed its inherent beta crystal structure, showing intense peaks at 7.92° and 22.7° 2Θ. The incorporation of Zr atoms into Si-Beta via SSIE did not affect its crystal structure, showing a similar XRD pattern to that of the parent Si-Beta. Importantly, there was no appearance of the typical bulk ZrO_2 peaks at 25°, 50°, and 60° 2Θ, suggesting the complete incorporation of Zr atoms into the beta framework (5 wt%) [35]. In addition, the XRD pattern of Zr-Beta remained unchanged after the impregnation of HPA. There were no XRD peaks related to the Keggin-structure of HPW and HSiW at 8–10°, 22°, 27°, and 35° 2Θ, possibly due to the low loading amounts of HPAs onto the Zr-Beta (< 2 wt%) [36,37].

The existence of both Zr and HPA components on the HPA/Zr-Beta was confirmed through compositional analysis by ICP and XPS (see Table 1). Especially, the bulk and surface Zr contents of the Zr-Beta were similar to each other (4.1 vs 5 wt%), suggesting that the Zr atoms
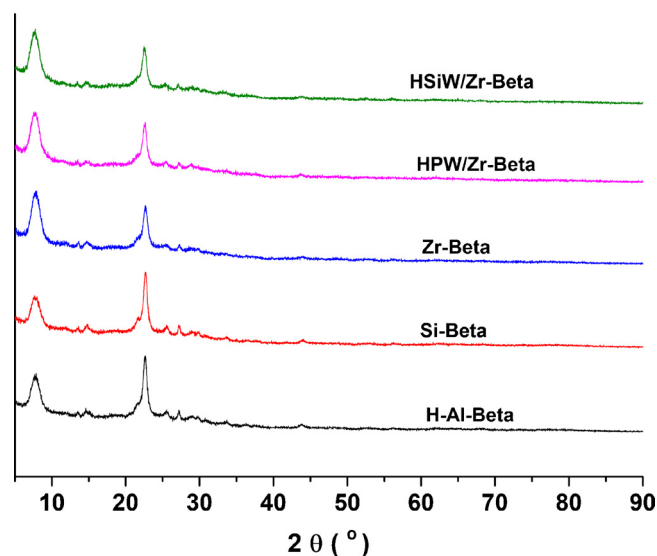

Fig. 1. XRD spectra of the prepared catalysts.

Table 1
Physicochemical properties of the prepared catalysts.

Catalyst	S_{BET}[1] (m^2/g)	V_{total}[1] (cm^3/g)	Zr ([a]Al) loading[2] (% wt)	HPA loading (% wt)	Total acidity[3] (mmol/g)	BA/LA[4]
H-Al-Beta	546	1.05	([a]3.7)	0.0	0.92	1.94
Si-Beta	573	1.22	([a]0.06)	0.0	0.03	0.08
Zr-Beta	506	1.01	4.1[a] (5)[b]	0.0	0.37	0.12
HPW/Si-Beta	497	1.07	0.0	1.50[a](0.40)[b]	0.32	n.a.
HPW/Zr-Beta	467	0.89	4.8[b]	1.50[a](1.1)[b]	0.78	0.31
HSiW/Si-Beta	505	1.16	0.0	1.60[a](0.50)[b]	0.34	n.a.
HSiW/Zr-Beta	488	0.89	5.7[b]	1.60[a](1.1)[b]	0.71	0.28

[a] BA/LA : Brønsted /Lewis ratio.
[1] Measured by using N_2-physisorption technique.
[2] Compositional analysis measured by ([a]ICP and [b]XPS techniques).
[3] Measured by NH_3-TPD.
[4] Measured by pyridine-adsorbed FTIR technique.

Fig. 3. DR-UV Vis spectra of the prepared catalysts.

are embedded onto the dealuminated beta framework uniformly. Meanwhile, the W contents measured by the ICP and XPS techniques exhibited larger differences in both the HPW/Zr-Beta and HSiW/Zr-Beta (1.6 vs 1.1 wt%), indicating that the distribution of the HPAs are less uniform compared to the Zr atoms. This difference can be attributed to the formation of large aggregates of HPA molecules on the surface of the zeolite beta. In order to examine the distribution of Zr and HPAs on the surface of zeolite beta in detail, STEM-EDS analyses were also performed. The SEM-EDS mapping images of the HPA/Zr-Beta showed that both the Zr and W were fairly homogeneously dispersed on the zeolite surface (Fig. 2).

The textural properties of the prepared catalysts were also examined using N_2-physisorption analysis, as shown in Table 1. The dealumination of H-Al-Beta resulted in a slight increase in both the BET surface area and total pore volume as expected. Meanwhile, the addition of Zr atoms and HPA molecules to Si-Beta led to a progressive decrease in the BET surface area and total pore volume. Between HPA and Zr, HPA caused a reduction in the pore volume to a greater extent, despite its low loading amount (1.6 wt% vs 5 wt%). This phenomenon can be explained by the bulkiness of the HPA structure (10 Å for its primary structure) which is larger than the pore window size of zeolite
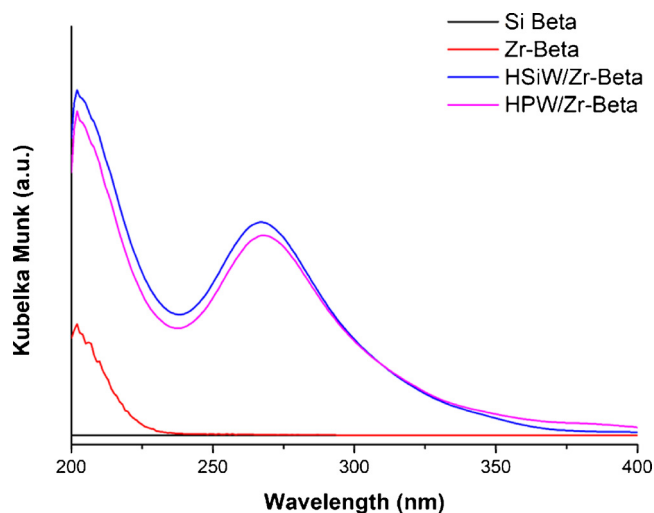
beta (~6 Å) [38,39]. HPA molecules are likely located in the exterior surface of Zr-Beta zeolite, partially blocking the micropore openings and resulting in the reduction of the pore volume.

HPA loaded Zr-Beta zeolites were further characterized using DR-UV–vis and XPS techniques to determine the chemical and electronic state of the incorporated Zr and HPA molecules. Fig. 3 shows the UV–vis spectra of the Zr-Beta and HPA/Zr-Beta zeolites. Zr-Beta exhibited a single distinct peak at 202 nm which can be assigned to the tetrahedral Zr^{4+} ions bonded to the zeolite framework through oxygen linkages [32]. Importantly, there was no reflectance peak around the 230 nm region which is ascribed to the charge transfer from the Zr-O-Zr bonds, indicating the absence of any bulk ZrO_2 phase in the catalyst [33]. In the case of the HPA loaded Zr-Beta zeolites, an additional intense peak was observed at 260 nm, which is the characteristic band of the Keggin-type heteropolytungstates, together with a peak at 202 nm [40]. Overall, the UV-VIS spectra of the HPA/Zr-Beta indicate that the Zr atoms are well incorporated into the zeolite beta framework with tetrahedral coordination, and the Keggin structure of the HPA is well preserved on the surface of the Zr-Beta.

Fig. 4 shows the Zr 3d and W 4f XPS spectra of the prepared catalysts. Regarding the Zr 3d spectra, the reference bulk ZrO_2 exhibited two distinct peaks at 181.9 and 184.3 eV corresponding to Zr 3d$_{5/2}$ and

Fig. 2. SEM-EDS mapping images of the prepared catalysts.
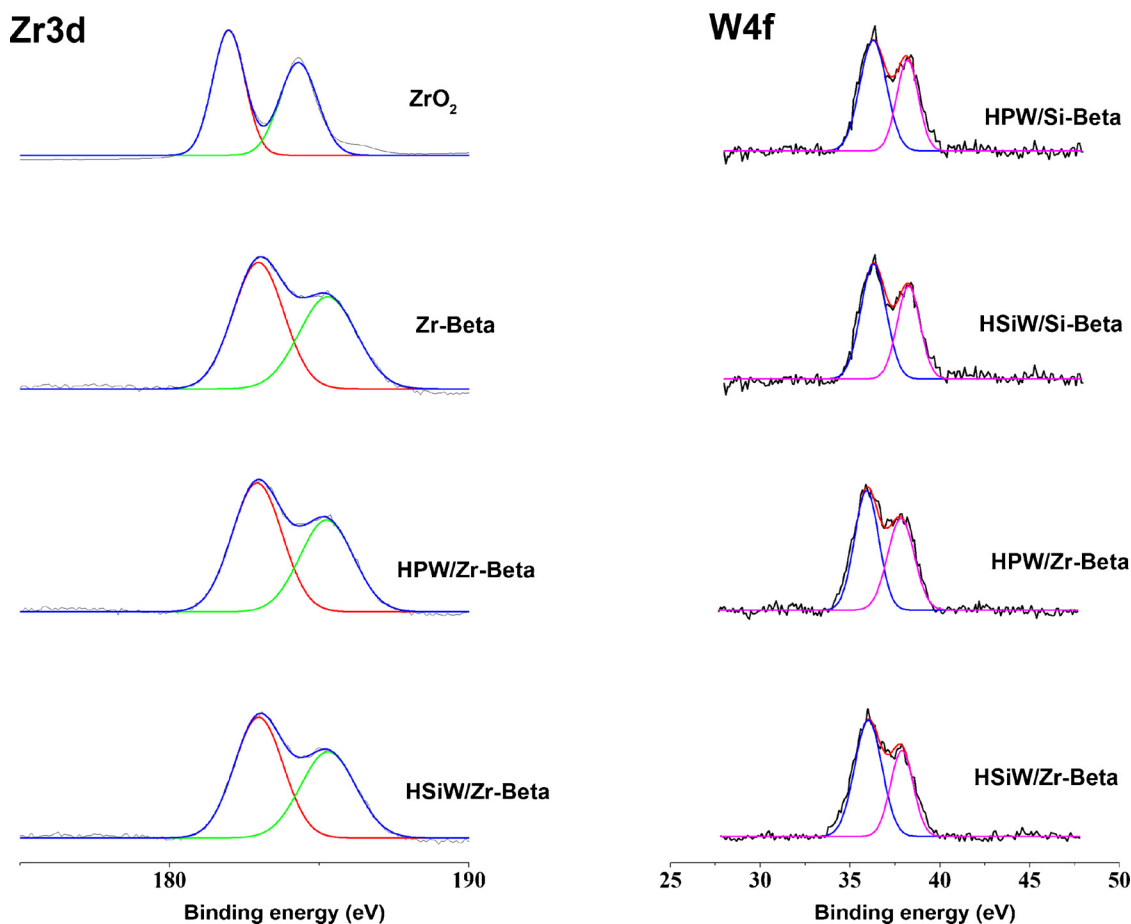
Fig. 4. Zr 3d (Left) and W 4f (Right) XPS spectra of the prepared catalysts.

Zr $3d_{3/2}$, respectively. For Zr-Beta, these peaks shifted toward the higher binding energy values of 183 and 185.3 eV, indicating the tetrahedral incorporation of the Zr atoms into zeolite framework, forming the Si-O-Zr bonds [33]. The observed binding values for the prepared Zr-Beta were in good agreement with those of the tetrahedral Zr species reported in the literature [9]. In addition, the impregnation of HPA (HPA/Zr-Beta) did not alter the electronic state of the Zr species, showing the same binding energy values with the Zr-Beta. This suggests that the Zr sites are atomically separate from the HPA molecules within the HPA/Zr-Beta. Regarding the W 4f spectra, the HPA loaded Zr-Beta showed two peaks at 36.3 and 38.3 eV corresponding to the W $4f_{7/2}$ and W $4f_{5/2}$ core level of W^{6+} ions, respectively [41]. These binding energy values were pretty similar to those of the silica-supported heteropolytungstates reported in the literature, indicating that the heteropolyanions are mainly bound to the silica matrix (not zirconium), thereby resulting in the weak metal-support (zeolite beta matrix) interaction [42]. Overall, based on the UV-VIS and XPS results, it is concluded that both SSIE for Zr incorporation and incipient wetness for HPA incorporation successfully anchored the intended active sites onto the zeolite beta matrix.

Because the most important aspect for one-pot furfural conversion into GVL is the catalyst acidity, the effects of the Zr and HPA addition toward the acid properties of the catalysts were studied in detail using various probe molecules. Table 1 shows the surface acidity of the prepared catalysts measured by ammonia-TPD. The total acidity of the parent Al-Beta decreased significantly from 0.92 to 0.03 mmol NH_3/g after the Al removal process as expected. Meanwhile, the addition of Zr atoms increased the total acidity from 0.03 to 0.37 mmol NH_3/g, indicating that the incorporated Zr atoms provide new acid sites with an 8.29 mmol NH_3 uptake per 1 g-Zr atom. Moreover, the addition of HPW

and HSiW to the Zr-Beta further increased the total acidity to 0.78 and 0.71 mmol NH_3/g, respectively. The acidity increase with the HPA addition was higher than that with the Zr addition despite their low loading amounts (< 1.5 wt%). In addition, the NH_3-TPD profiles of the catalysts indicated a clear difference in the acid strength between the acid centers of the Zr and HPA (see Fig. 5). While the Zr-Beta exhibited
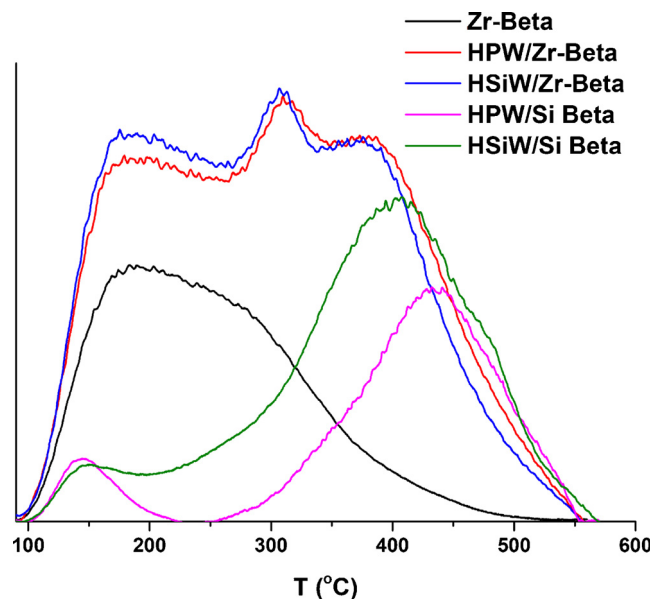

Fig. 5. NH_3-TPD profiles of Zr-Beta and HPA loaded samples.

a broad desorption peak centered at a low temperature of 443 K, the HPA loaded Si-Beta showed an intense desorption peak at > 673 K together with a small peak at < 423 K, indicating that HPA has stronger acidity than the framework Zr site. In the case of the HPA loaded Zr-Beta, there existed three distinct desorption peaks centered at 443, 598 and 663 K, indicating the presence of both weak and strong acid sites. The peaks at 443 and 663 K could be attributed to the desorption of NH_3 molecules from the framework Zr and HPA sites, respectively. In contrast, the appearance of a new desorption peak at 598 K (medium acid strength) indicates the formation of new acid sites on the surface of the HPA/Zr-Beta such as fragmented Keggin units.

The nature and distribution of the acid sites induced by the Zr and HPA addition were further probed with pyridine-FTIR. Table 1 shows the ratio of the Brønsted to Lewis acid sites (BA/LA) of the catalysts measured by pyridine-FTIR. After the dealumination process, the BA/LA ratio of the Al-Beta decreased significantly from 1.94 to 0.08. Meanwhile, the addition of Zr to the dealuminated beta framework increased the BA/LA ratio from 0.08 to 0.12 and the total acidity from 0.03 to 0.37 mmol NH_3/g. This indicates that the Zr addition induces both Lewis and weak-Brønsted acid sites on the catalyst surface, even though Zr-Beta was previously regarded as a purely Lewis acid catalyst. The weak Brønsted acidity of the Zr-Beta sample likely arises from the $Zr-OH$ hydroxyl groups formed by the partial hydrolysis of the Zr-O-Si bond [43,44] or neighboring silanol groups [45], while tetrahedrally coordinated Zr species act as a Lewis acid center. In the Zr-Beta zeolite, partially hydrolyzed lattice Zr sites of $Zr(OSi)_3OH$ were reported to be the main active sites for the MPV reaction [43]. Although the catalysis of the $Zr-OH$ hydroxyl or silanol sites is not well understood, they are thought to act as weak Brønsted acid sites. On the other hand, the addition of HPW and HSiW to Zr-Beta improved the BA/LA ratio from 0.12 to 0.31 and 0.28, respectively, due to the purely Brønsted acidic character of Keggin HPAs. The NH_3-TPD results of the HPA loaded Zr-Beta also indicated that the addition of HPA to Zr-Beta resulted in the appearance of new acid sites with medium strength together with strong acid sites. Therefore, these results suggest that the addition of HPA to Zr-Beta results in the formation of both Brønsted and Lewis acid sites, which originate from the Keggin HPAs bound to the silica matrix and the fragmented Keggin structure, respectively. Despite their structure similarity, HPW and HSiW affect the BA/LA ratio in a slightly different manner. One possible explanation of this phenomenon can be the difference in the Brønsted acid strength between HPW and HSiW.

Overall, the addition of Zr and HPA to Si-Beta led to a progressive increase in the total acidity of the catalysts, and the observed NH_3-TPD profiles indicate that the HPA and Zr active sites do not interfere with each other. The presence of both strong Brønsted and Lewis acid sites in the HPA loaded Zr-Beta was also confirmed by pyridine-FTIR analysis.

3.2. Intrinsic catalytic activity of the HPA loaded Zr-Beta catalysts

Based on previous reports [13,23], a possible reaction scheme for the one-pot conversion of furfural to GVL over the bifunctional Lewis/Brønsted acid zeolites is depicted in Fig. 6. In the first step, furfural is converted into FA via transfer hydrogenation over the Lewis acid sites using 2-propanol as a hydrogen donor. FA is subsequently etherified to FE promoted by both the Lewis and Brønsted acids. Next, FE is converted into IPL through the hydrolytic ring-opening reaction over the Brønsted acid sites. In parallel, FE or FA can initially be converted into angelica lactone (AL) and then hydrolyzed into LA and its ester. Finally, IPA undergoes the second transfer hydrogenation to produce isopropyl 4-hydroxypentanoates over Lewis acid sites followed by lactonization to form GVL.

To examine the catalytic activity of the individual Zr and HPA sites for the intended reactions and to check if there is any interaction between the two sites within the same catalyst, the conversion of several key intermediates was initially studied using the prepared catalysts. Fig. 7 shows the catalysis results for the conversion of FA over various

metal (Al or Zr) and HPA-containing zeolite catalysts. The reactions were conducted at 413 K in a short reaction time (1.5 h) to measure the initial activity of the catalysts (< 30% conversion). Because the conversion of FA mainly involves the hydrolytic-ring opening reaction forming LA or IPL, it is a suitable reaction for studying the intrinsic activity of the Brønsted acid sites in the catalysts. The results showed that Si-Beta with almost no Brønsted acid sites exhibited a very high FE production rate (0.85 mmol/h) along with a low IPL production rate (0.03 mmol/h). Meanwhile, the addition of HPA to Si-Beta resulted in a decrease in the FE production rate (0.55-0.63 mmol/h) and in a significant increase in the IPL production rate (0.26-0.28 mmol/h), indicating that the HPA addition leads to the formation of strong Brønsted acid sites. Importantly, compared to the conventional Al-Beta, HPA was more selective toward the formation of IPL and had a lower AL production rate. Although AL can be converted into IPL over Brønsted acids (see Fig. 6), our previous investigation revealed that the conversion of AL to IPL is extremely slow and energy-intensive [23]. Therefore, this result suggests that HPA is a more effective catalyst for promoting the hydrolytic ring-opening reaction than that of the Al-Beta, possibly due to its stronger Brønsted acidity [46].

Zr-Beta zeolite also showed some activity in the production of IPL and FE, but its activity was significantly lower than those of the HPA/Si-Beta. This suggests that the weak Brønsted acid sites of the Zr-Beta cannot efficiently promote the hydrolytic ring-opening reaction of FA. The addition of HPA to the Zr-Beta enhanced the IPL production rate significantly from 0.03 to 0.12 mmol/h, indicating that the added HPA molecules well function as Brønsted acid sites. However, their rates were somewhat lower than those of the HPA loaded onto the Si-Beta despite the identical HPA loading. This result implies that some of the HPA molecules lose their Brønsted acidity due to the decomposition of the Keggin structure on the surface of the Zr-Beta, as evidenced by the NH_3-TPD and Py-FTIR results. Interestingly, the production rates of FE, AL, and IPL are similar in Zr-Beta and Si-Beta. This can be explained by the similar BA/LA ratio between Si-Beta and Zr-Beta as shown in Table 1. Despite the significant increase in the total acidity after Zr-atoms addition, anchored Zr-active sites act mainly as Lewis acid sites. From the results of our previous study, Lewis acid catalyst was proven to have low activity toward the hydrolytic ring-opening of FA, whereas it has good activity for the etherification reaction of FA. Therefore, it can be suggested that both weak-Brønsted acid and Lewis acid sites are less active for catalyzing the hydrolytic ring-opening reaction of FA.

Next, the MPV reduction of LA was studied to investigate the Lewis acidity of the added Zr atoms in the catalysts, as shown in Fig. 8. The results showed that the Zr-Beta was capable of producing GVL and IPL, indicating that the incorporated Zr atoms well function as isolated Lewis acid sites, promoting the MPV reduction. Compared to the Zr-Beta, the HPA loaded Zr-Beta showed a significantly enhanced GVL production rate. The rate of GVL production increased from 0.09 mmol/h for the Zr-Beta to 0.3 mmol/h for the HPA/Zr-Beta. The higher GVL production rate over the HPA/Zr-Beta is likely attributed to the enhanced esterification of LA to IPL over Brønsted acid sites, because the MPV of IPL is more energetically favorable than that of LA [23]. Overall, these results suggest that the activity of the Zr sites for the MPV reaction remains intact after the addition of HPA to Zr-Beta.

3.3. Effect of the Zr and HPA loading amounts

To optimize the catalytic performance of the bifunctional HPA/Zr-Beta catalyst for GVL production, the loading amounts of Zr and HPA need to be well balanced. Therefore, the loading amounts of the Zr and HPA on Si-Beta were varied, and their impacts on the rates of the MPV reduction and hydrolytic ring-opening were investigated in detail. When the Zr loading amount on the Si-Beta was changed from 2.5 to 10 wt%, the GVL production rate from LA showed a volcano-type behavior with a maximum rate of 0.09 mmol/h at a 5 wt% loading (Table S1). This can be explained by the fact that the number of free silanol
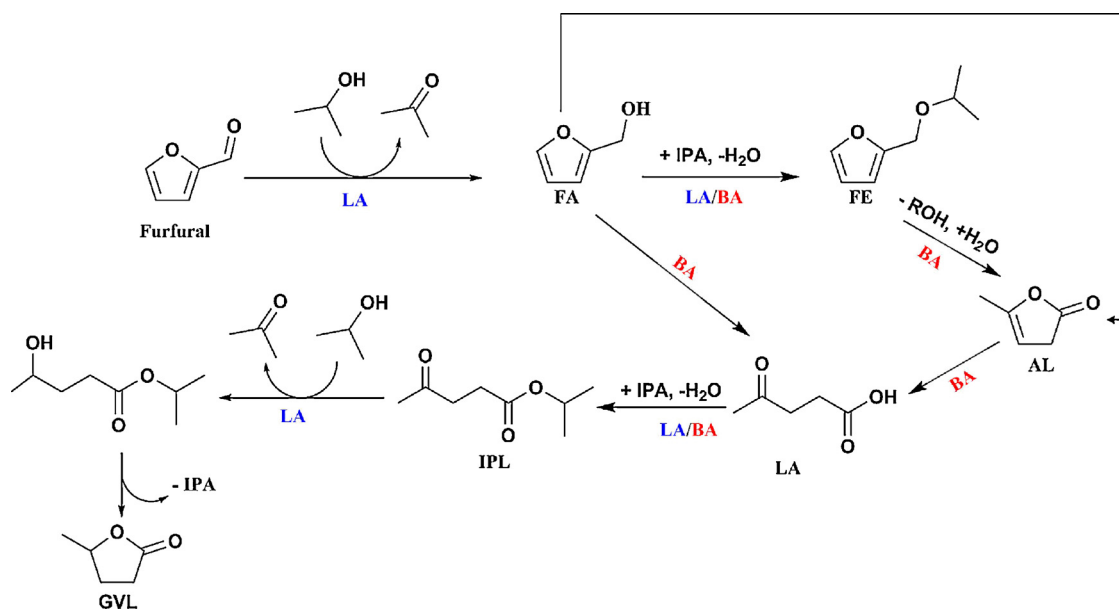
Fig. 6. Reaction network for the conversion of furfural to GVL.

nests for the incorporation of the tetravalent Zr active sites in the dealuminated beta matrix only take up 5 wt% Zr. Thus, an increase in the Zr loading beyond 5 wt% can result in the formation of bulk ZrO_2 and pore blockage, thereby decreasing the MPV activity of the catalyst. In the case of the HPA, the optimum loading of the HPA on the Zr-Beta was found to be 2 wt% (the ICP measured values were around ~1.6%). When the HPW loading amount was increased from 2 to 4 wt%, the IPL production rate from FA decreased from 0.13 to 0.11 mmol/h, indicating that a higher HPW loading did not lead to an increase in the proton site density on the catalyst surface (Table S2). More importantly, the GVL production rate from LA significantly decreased from 0.29 to 0.19 mmol/h when the HPW loading amount was increased (Table S3), suggesting that a higher HPW loading even results in a decrease in the rate of MPV reduction over the Zr sites. This can be attributed to the decreased accessibility of the reactants to the Zr active sites inside the micropores caused by pore blockage from the bulky Keggin HPA units. Overall, the optimum loading amounts of the HPA and Zr in the HPA/
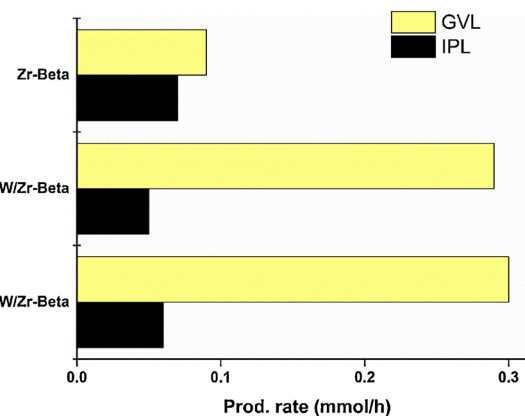

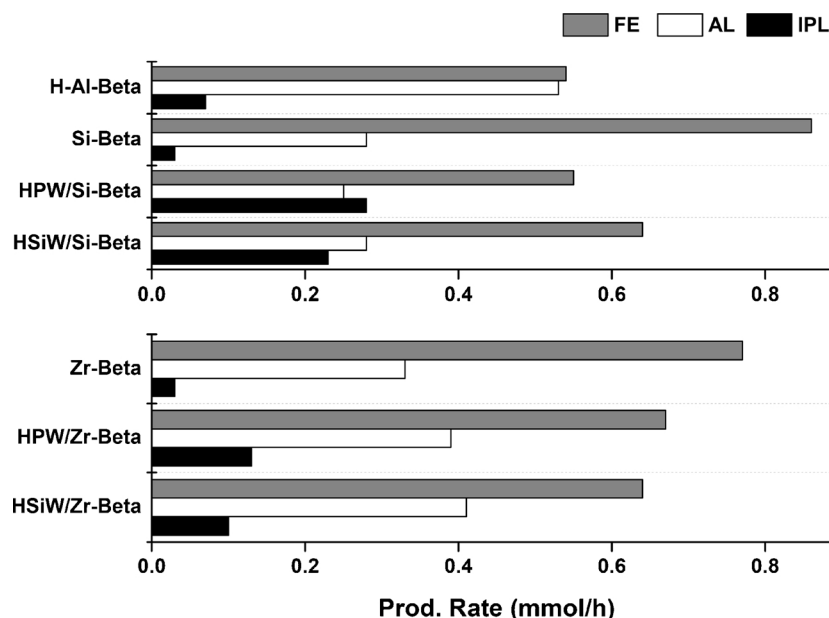**Fig. 8.** Production rates of GVL and IPL measured from LA conversion.

Fig. 7. Production rates of several intermediates measured from FA conversion.
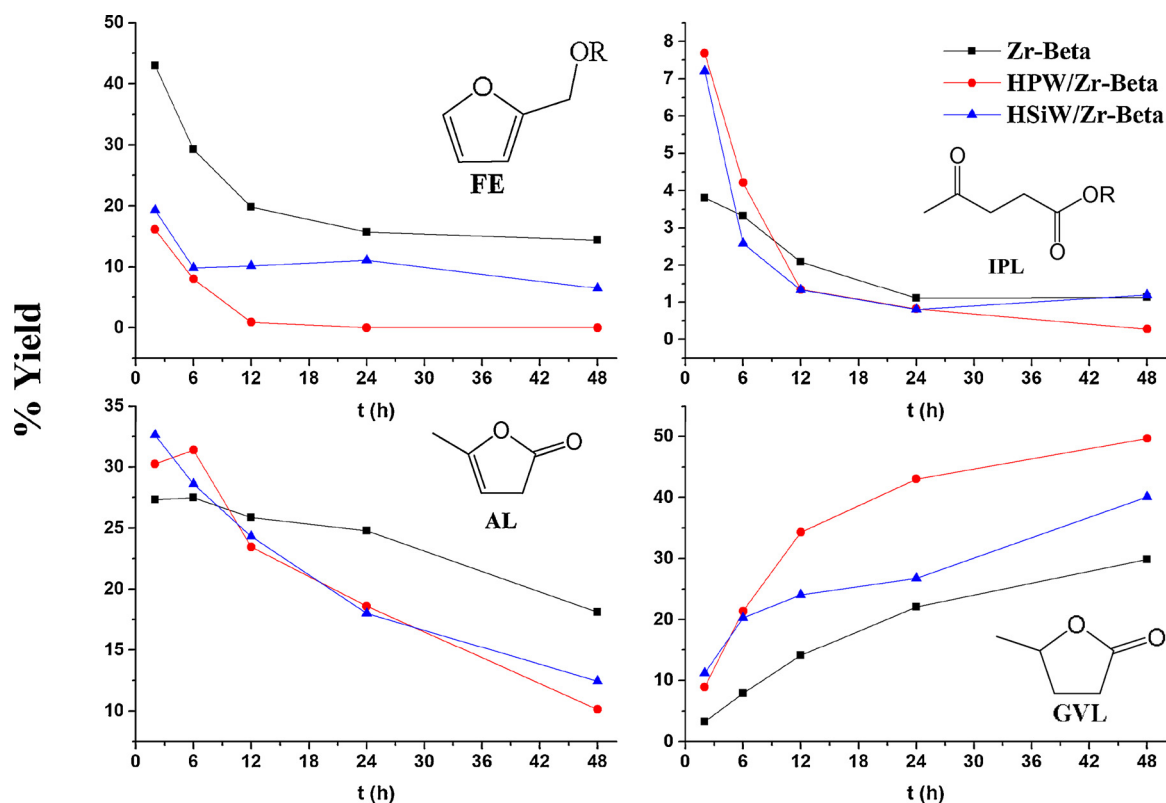
Fig. 9. Product yields as a function of time at 413 K.

Zr-Beta catalyst were determined to be 2 and 5 wt%, respectively. In addition, the effect of the initial metal loading amounts on the acidity distribution (i.e., the ratio of Brønsted and Lewis acid sites) and its correlation with the production rates of targeted intermediates were further examined (see Fig. S2). Both IPL and GVL production rates showed a volcano-type behavior with a maximum value at the medium Brønsted-to-Lewis acid ratio (B/L) of ~0.3, and 2% HPA/5% Zr-Beta possessed the optimum B/L ratio. Therefore, the aforementioned HPW/ Zr initial loading ratio was used as a basis to prepare the catalysts for further experimental activities.

3.4. Conversion of furfural into GVL

The optimized HPA loaded Zr-Beta zeolites with 2 wt% HPA and 5 wt% Zr loading amounts were finally applied to the one-pot conversion of furfural to GVL. The reactions were carried out at 413 K in 2-propanol with a catalyst to furfural ratio of 0.4. Fig. 9 shows the yields of GVL and the intermediates as a function of the reaction time (2–48 h) over the Zr-Beta and HPA/Zr-Beta zeolites. The conversion of furfural reached ~100% within 2 h for all the catalysts (data not shown). However, the GVL production rates over the HPA loaded Zr-Beta zeolites (HPW and HSiW) were considerably higher than that over the Zr-Beta. The final GVL yield over the HPW/Zr-Beta reached ~50% after 48 h, whereas that over the Zr-Beta only reached ~27%. The reaction profiles also clearly indicate that the initial reaction products, i.e., FE and AL, are consumed more slowly over the Zr-Beta zeolite due to the absence of strong Brønsted acidity. Between the HPW/Zr-Beta and HSiW/Zr-Beta, the HPW loaded one exhibited a superior activity for GVL production (50% vs 40% final GVL yield), even though they had a similar number and distribution of acid sites (Table 1). Given that the initial GVL formation rate over the HSiW/Zr-Beta is pretty similar to that over the HPW/Zr-Beta, the lower final yield of GVL over the HSiW/ Zr-Beta can be attributed to the lower stability of the HSiW anchored on the Zr-Beta, resulting in loss of active sites by sintering or leaching. This

hypothesis is also supported by the significantly decreased activity of the HSiW/Zr-Beta over extended reaction time for the hydrolytic ring-opening of FE as shown in Fig. 9. Overall, the bifunctional HPA loaded Zr-Beta catalysts with both isolated Lewis and Brønsted acid sties demonstrated their superiority in the one-pot production of GVL from furfural over a single Zr-Beta catalyst. Especially, the HPW/Zr-Beta exhibited a better performance for the overall production of GVL than that of the HSiW loaded one.

To maximize the GVL yield, the reaction conditions were optimized using the best performing HPW/Zr-Beta catalyst. The catalytic results of the one-pot conversion of furfural over the HPW/Zr-Beta at various temperatures are listed in Table 2. For these runs, the catalyst to furfural ratio was increased to 1, and the reaction time was fixed at 24 h. The results showed that the GVL yield increased from 54.3% to 67.9%, and the AL yield decreased from 14.5% to 1.7% with an increase in the reaction temperature from 393 to 433 K, indicating that a higher

Table 2
Catalytic performances of HPW/Zr-Beta catalysts for GVL production at various conditions.

Catalyst	Temp (K)	Y_{GVL} (mol%)	Y_{AL} (mol%)	Y_{IPL} (mol%)	Y_{FAC} (mol%)	$Y_{DI\,Ether}$ (wt%)
HPW/Zr-Beta	393	54.3	14.5	1.8	2.0	2.1
HPW/Zr-Beta	413	61.0	3.4	1.7	1.7	8.0
HPW/Zr-Beta	433	68.0	1.7	1.0	0	8.5
Sn-Al-Beta [23]	433	43.2	28.8	4.0	0	3.3
Spent-Washed[a]	433	48.6	1.3	0.4	0.9	2.8
Spent-Calcined[b]	433	60.7	0	3.0	0.5	4.3
Spent-Calcined[c]	433	68.5	0	0.5	0.3	7.0

[a] After reaction, the spent catalyst was collected, washed with acetone, dried in oven and then reused for the next reaction.
[b] The spent catalyst was washed, dried, and calcined under air flow at 623 K for 4 h.
[c] The spent catalyst was washed, dried, and calcined under air flow at 773 K for 4 h.

temperature can promote the hydrolytic ring-opening of AL, thereby enhancing the GVL yield. In addition, the highest GVL yield obtained in this study surpassed that over the conventional Sn-Al-Beta catalyst under the same condition in our previous work (68% vs 43%). The additional comparison of two catalysts at low temperature (~393 K) and short reaction time (6 h) also demonstrated that the activity of HPW/Zr-Beta outperformed that of Sn-Al-Beta in terms of the rates of both MPV and ring-opening reactions under the conditions similar to other researches (see Table S7). Importantly, the HPW/Zr-Beta was capable of achieving a high GVL yield at low temperatures (< 413 K) due to its enhanced BrØnsted acid strength. In addition to the furfural-derived products, Table 2 shows the yield of diisopropyl ether, which are produced by the self-etherification of IPA solvent. The yield of diisopropyl ether was observed to increase with increasing temperature and the use of HPW/Zr-Beta. Multiple studies have shown that higher temperatures and stronger acidity accelerate the etherification of alcohols [48,49].

The effect of other reaction parameters, i.e., the reactant-to-catalyst (R/C) ratio and initial furfural concentration, on the final GVL yield were also examined, and the results are shown in Tables S4 and S5, respectively. It is important to maintain the high GVL yield at a high R/C ratio and a high furfural concentration in order to make the developed catalyst industrially viable. The results showed that the final GVL yield was not changed significantly by the variation of the R/C ratio and initial furfural concentration, and the high-yield production of GVL (> 60%) was possible under the industrially-relevant conditions (the R/C ratio of ~2.5 and the initial furfural concentration of ~0.34 M), highlighting the effectiveness of HPW/Zr-Beta as a catalyst for the integrated conversion of furfural to GVL.

Lastly, the stability and reusability of the HPW/Zr-Beta was investigated. For this purpose, the spent catalyst was recovered through centrifugation, washed with acetone, and then retested for the furfural conversion. The reused catalyst exhibited a lower GVL yield than the fresh catalyst (49%), indicating loss of some active sites even after 1st reaction (see Table 2). Previous studies have shown that the formation of coke on the catalyst surface is the main cause of catalyst deactivation during the one-pot conversion of furfural to GVL over solid acid catalysts [13,23,47]. The TGA analysis of the spent HPW/Zr-Beta confirmed that a considerable amount of carbon (~15 wt%) was deposited on the catalyst (Fig. S1). Meanwhile, ICP studies with product solution revealed that leaching of HPW was negligible. Therefore, the spent catalyst was subjected to calcination at high temperatures (> 573 K) for its regeneration. The catalysis results showed that the initial activity of the catalyst was completely regained after calcination at 773 K, reaching ~68% GVL yield. Thus, these results suggest that the HPW/Zr-Beta is reusable after calcination in air.

4. Conclusions

In summary, the use of Keggin heteropolyacid (HPA) in providing BrØnsted acid sites over Zr-Beta zeolite is an effective method for creating both isolated Lewis and BrØnsted acid sites in a single zeolite catalyst. The characterization studies of the catalysts using XRD, BET, UV–vis and XPS indicate that the Keggin structures of the added phosphotungstic acid (HPW) and silicotungstic acid (HSiW) are well preserved on the surface of the Zr-Beta, and they are atomically separate from Zr in the zeolite matrix. Results from the TPD of ammonia and FT-IR spectroscopy of the adsorbed pyridine clearly demonstrate that the HPA/Zr-Beta possesses well-defined Lewis and BrØnsted acid sites. When the HPA/Zr-Beta catalysts are applied to the one-pot conversion of furfural to GVL, they demonstrate much higher yields of GVL compared to Zr-Beta due to the increased rate of hydrolytic ring-opening reaction promoted by the BrØnsted acid sites, while the transfer hydrogenation of furfural and levulinic acid (LA) are well catalyzed by the Lewis acid sites provided by the intact framework Zr sites in the catalyst. Especially, the HPW loaded Zr-Beta exhibits a remarkable catalytic

performance for GVL production (~70 mol%) at 433 K after 24 h due to its high thermal stability and stronger BrØnsted acidity, and its activity far surpasses that of the conventional Sn-Al-Beta zeolite. Overall, the use of HPA as the source of BrØnsted acidity for Lewis acid Sn- or Zr-Beta zeolites is proven to be a viable alternative to the internal Al atoms for an efficient one-pot production of GVL from furfural. The bifunctional HPA/Zr-Beta catalyst developed in this study would be applicable to a range of biomass conversion processes that require both acid and reduction chemistry.

Conflicts of interest

There are no conflicts of interest to declare.

Appendix A. Supplementary data

Supplementary material related to this article can be found, in the online version, at doi:https://doi.org/10.1016/j.apcatb.2018.09.031.

References

[1] G.W. Huber, S. Iborra, A. Corma, Chem. Rev. 106 (2006) 4044–4098.
[2] V. Mendu, T. Shearin, J.E. Campbell, J. Stork, J. Jae, M. Crocker, G. Huber, S. DeBolt, Proc. Natl. Acad. Sci. U. S. A. 109 (2012) 4014–4019.
[3] R. Xing, W. Qi, G.W. Huber, Energy Environ. Sci. 4 (2011) 2193–2205.
[4] M. Yabushita, H. Kobayashi, A. Fukuoka, Appl. Catal. B 145 (2014) 1–9.
[5] L. Negahdar, I. Delidovich, R. Palkovits, Appl. Catal. B 184 (2016) 285–298.
[6] X. Zhang, D. Zhang, Z. Sun, L. Xue, X. Wang, Z. Jiang, Appl. Catal. B 196 (2016) 50–56.
[7] R. Xing, A.V. Subrahmanyam, H. Olcay, W. Qi, G.P. van Walsum, H. Pendse, G.W. Huber, Green Chem. 12 (2010) 1933–1946.
[8] D.M. Alonso, S.G. Wettstein, J.A. Dumesic, Green Chem. 15 (2013) 584–595.
[9] S. Song, L. Di, G. Wu, W. Dai, N. Guan, L. Li, Appl. Catal. B 205 (2017) 393–403.
[10] Y.T. Cheng, J. Jae, J. Shi, W. Fan, G.W. Huber, Angew. Chem. Int. Ed. 51 (2012) 1387–1390.
[11] Y.P. Wijaya, H.P. Winoto, Y.-K. Park, D.J. Suh, H. Lee, J.-M. Ha, J. Jae, Catal. Today 293-294 (2017) 167–175.
[12] K. Yan, Y. Yang, J. Chai, Y. Lu, Appl. Catal. B 179 (2015) 292–304.
[13] L. Bui, H. Luo, W.R. Gunther, Y. Román-Leshkov, Angew. Chem. Int. Ed. 52 (2013) 8022–8025.
[14] F. Li, L.J. France, Z. Cai, Y. Li, S. Liu, H. Lou, J. Long, X. Li, Appl. Catal. B 214 (2017) 67–77.
[15] M.J. Gilkey, B. Xu, ACS Catal. 6 (2016) 1420–1436.
[16] M. Chia, J.A. Dumesic, Chem. Commun. 47 (2011) 12233–12235.
[17] J. Song, L. Wu, B. Zhou, H. Zhou, H. Fan, Y. Yang, Q. Meng, B. Han, Green Chem. 17 (2015) 1626–1632.
[18] M. Koehle, R.F. Lobo, Catal. Sci. Technol. 6 (2016) 3018–3026.
[19] M.M. Villaverde, T.F. Garetto, A.J. Marchi, Catal. Commun. 58 (2015) 6–10.
[20] J. Wang, S. Jaenicke, G.-K. Chuah, RSC Adv. 4 (2014) 13481–13489.
[21] J. Jae, E. Mahmoud, R.F. Lobo, D.G. Vlachos, ChemCatChem 6 (2014) 508–513.
[22] M.M. Antunes, S. Lima, P. Neves, A.L. Magalhães, E. Fazio, A. Fernandes, F. Neri, C.M. Silva, S.M. Rocha, M.F. Ribeiro, M. Pillinger, A. Urakawa, A.A. Valente, J. Catal. 329 (2015) 522–537.
[23] H.P. Winoto, B.S. Ahn, J. Jae, J. Ind. Eng. Chem. 40 (2016) 62–71.
[24] B. Hernandez, J. Iglesias, G. Morales, M. Paniagua, C. Lopez-Aguado, J.L. Garcia Fierro, P. Wolf, I. Hermans, J.A. Melero, Green Chem. 18 (2016) 5777–5781.
[25] S. Zhu, Y. Cen, J. Guo, J. Chai, J. Wang, W. Fan, Green Chem. 18 (2016) 5667–5675.
[26] J.A. Melero, G. Morales, J. Iglesias, M. Paniagua, C. López-Aguado, K. Wilson, A. Osatiashtiani, Green Chem. 19 (2017) 5114–5121.
[27] I.V. Kozhevnikov, Chem. Rev. 98 (1998) 171–198.
[28] W. Alharbi, E.F. Kozhevnikova, I.V. Kozhevnikov, ACS Catal. 5 (2015) 7186–7193.

[29] J.K. Kim, J.H. Choi, J.H. Song, J. Yi, I.K. Song, Catal. Commun. 27 (2012) 5–8.
[30] A.M. Alsalme, P.V. Wiper, Y.Z. Khimyak, E.F. Kozhevnikova, I.V. Kozhevnikov, J. Catal. 276 (2010) 181–189.
[31] L. Frattini, M.A. Isaacs, C.M.A. Parlett, K. Wilson, G. Kyriakou, A.F. Lee, Appl. Catal., B 200 (2017) 10–18.
[32] P. Wolf, C. Hammond, S. Conrad, I. Hermans, Dalton Trans. 43 (2014) 4514–4519.
[33] B. Tang, W. Dai, X. Sun, G. Wu, N. Guan, M. Hunger, L. Li, Green Chem. 17 (2015) 1744–1755.
[34] S. Roy, K. Bakhmutsky, E. Mahmoud, R.F. Lobo, R.J. Gorte, ACS Catal. 3 (2013) 573–580.
[35] F. Gonell, M. Boronat, A. Corma, Catal. Sci. Technol. 7 (2017) 2865–2873.
[36] S.S. Kale, U. Armbruster, R. Eckelt, U. Bentrup, S.B. Umbarkar, M.K. Dongare, A. Martin, Appl. Catal., A 527 (2016) 9–18.
[37] I.V. Kozhevnikov, A. Sinnema, R.J.J. Jansen, K. Pamin, H. van Bekkum, Catal. Lett. 30 (1994) 241–252.
[38] S.R. Mukai, L. Lin, T. Masuda, K. Hashimoto, Chem. Eng. Sci. 56 (2001) 799–804.
[39] A.D. Newman, D.R. Brown, P. Siril, A.F. Lee, K. Wilson, Phys. Chem. Chem. Phys. 8 (2006) 2893–2902.
[40] T. Ma, J. Ding, R. Shao, W. Xu, Z. Yun, Chem. Eng. J. 316 (2017) 797–806.
[41] P.A. Jalil, M. Faiz, N. Tabet, N.M. Hamdan, Z. Hussain, J. Catal. 217 (2003) 292–297.
[42] X. You, L. Yu, F. Xiao, S. Wu, C. Yang, J. Cheng, Chem. Eng. J. 335 (2018) 812–821.
[43] M. Boronat, A. Corma, M. Renz, J. Phys. Chem. B 110 (2006) 21168–21174.
[44] V.L. Sushkevich, D. Palagin, I.I. Ivanova, ACS Catal. 5 (2015) 4833–4836.
[45] B.K. Chethana, S.H. Mushrif, J. Catal. 323 (2015) 158–164.
[46] M. Paniagua, J.A. Melero, J. Iglesias, G. Morales, B. Hernández, C. López-Aguado, Appl. Catal., A 537 (2017) 74–82.
[47] M.M. Antunes, S. Lima, P. Neves, A.L. Magalhães, E. Fazio, F. Neri, M.T. Pereira, A.F. Silva, C.M. Silva, S.M. Rocha, Appl. Catal. B 182 (2016) 485–503.
[48] I. Takahara, M. Saito, M. Inaba, K. Murata, Catal. Lett. 105 (2005) 249–252.
[49] W. Turek, J. Haber, A. Krowiak, Appl. Surf. Sci. 252 (2005) 823–827.